JEFFERSON LAB VERTICAL TEST AREA RF SYSTEM IMPROVEMENT*

T. Powers# and M. Morrone, Jefferson Lab, Newport News, VA, USA

Abstract

RF systems for testing critically coupled SRF cavities require the ability to track the cavity frequency excursions while making accurate measurements of the radio frequency (RF) signals associated with the cavity. Two types of systems are being used at Jefferson Lab. The first, the traditional approach, is to use a voltage controlled oscillator configured as a phase locked loop (VCO-PLL) such that it will track the cavity frequency. The more recently developed approach is to use a digital low level RF (LLRF) system in self excited loop (SEL) mode to track the cavity frequency. Using a digital LLRF system in SEL mode has the advantage that it is much easier to lock to the cavity's resonant frequencies and they tend to have a wider capture range. This paper will report on the system designs used to implement the 12 GeV digital LLRF system in the JLAB vertical test area. Additionally, it will report on the system modifications which are being implemented so that the RF infrastructure in the VTA will be ready to support the LCLS II cryomodule production effort, which is scheduled to begin in calendar year 2016.

INTRODUCTION

The JLAB Vertical test area (VTA) was originally constructed in 1990 [1]. It has eight vertical test dewars capable of being operating at temperatures down to 1.6 K. Six of the dewars have radiation shielding which allows one to safely test SRF structures which are capable of producing radiation. Two of the dewars, which are not shielded are used to test non accelerating structures at low temperatures. The VTA is supported by a helium liquefier, pumping and recovery system, which is dedicated to production testing of superconducting cavities and cryomodules. Over the past 25 years the facility has been used to perform in excess of 5,200 cavity tests on more than 600 different cavities.

The VCO-PLL based, L-band RF systems in the JLAB vertical test area (VTA) were built in the early 1990's and have worked well over the years [2]. An additional UHF system, with capabilities from 500 MHz to 1 GHz, was implemented in 2002 and used for production testing of the SNS cavities. In recent years one of the L-band systems has been dedicated to testing 1497 MHz cavities while the second has been used for testing 1300 MHz cavities. The 1497 MHz system has a high power switching network that routes the drive signals between the different test dewars and provides the appropriate personnel safety interlocks.

* Authored by Jefferson Science Associates, LLC under U.S. DOE Contract No. DE-AC05-06OR23177 with supplemental funding from the LCLS-II Project U.S. DOE Contract No. DE-AC02-76SF00515.
#powers@jlab.org

The first system that was upgraded to a digital LLRF based system was the UHF system. One of the driving factors for this upgrade was the failure of the vector modulator which was used to control the phase and amplitude of the output signal. Unfortunately, this part is no longer available and replacement with an analog input variant suffers from "dead zones" in phase and amplitude space when the attenuation is much above 20 dB. In addition to avoiding future failures of obsolete parts, the L-band systems are being upgraded in order to increase the frequency range to 1.2 GHz to 1.6 GHz as well as to improve the ease to test the cavities. We are also installing a switching network that will allow one to route the RF power to and RF signals from either of the two L-band systems to/from any of 6 shielded vertical test dewars.

RF HARDWARE CONFIGURATION

The L-band RF system consists of a pair of digital low level RF systems which are fed into a high power/low power amplifiers. The output of the amplifier networks are fed into a 2-input, 6-output RF switching network. The RF signals from the cavities are routed back to the measurement network through a set of three 6-input, 2-output low power RF switching networks. The overall block diagram is shown in Figure 1.

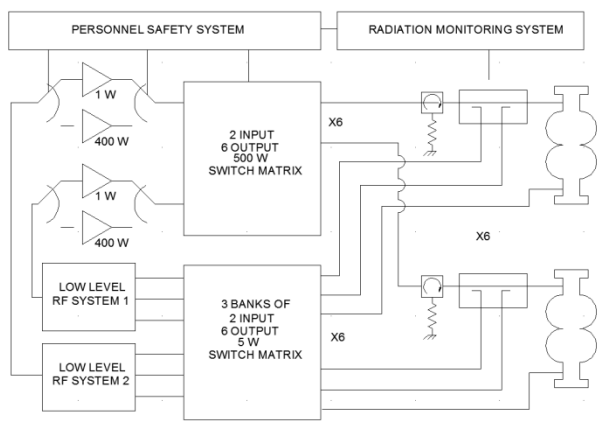

Figure 1: System level block diagram of a the L-Band system.

RF-Switching Networks

Two modified commercial off-the-shelf switching networks were procured for this system. Rather than a standard USB interface the coil signals and the high power RF-switch position read-back contact closures were brought out to connectors. This was done so that the system could be integrated into the personnel protection system which is implemented in a PLC. Had we used the USB interface there would have been issues with certification of the system to safety system standards. An

ISBN 978-3-95450-178-6

extra SPDT fail safe switch was inserted at each of the inputs of the high power network to ensure that the amplifier outputs were directed to a load in the event of a PSS system fault.

One of the RF topology changes that was implemented several years ago was the placement of the incident and reflected power directional coupler. In the original 1990 system design the topology was high/low power switching network, followed by a dual directional coupler followed by a single pole 8-throw switch which was used to direct the RF power to the selected cavity. This was done to reduce the number of cables in the system and the complexity of the switching network. Unfortunately, this introduced standing wave induced errors in the incident and reflected power measurements. In order to address this issue each of our production test dewars was equipped with a directional coupler, circulator and circulator load. With this arrangement, the forward and reflected power were routed to the measurement hardware via a patch panel. The new system will continue to use the circulator/load and directional coupler at each dewar location. However, the patch panel currently in use will be replaced with a bank of three 6-input 2-output modified commercial off the shelf RF-switching networks. One bank each for incident reflected and transmitted power. The control signals for these switches are connected in parallel with that of the high power network.

Frequency Tracking Low Level RF System

The digital low level RF system selected for this application is the JLAB Field Control Chassis (FCC), which was developed for 12 GeV upgrade [3]. We chose this unit because it met our needs, the required infrastructure was in place and, with a new receiver card, it could be used at several different frequencies. The standard JLAB receiver card uses a local oscillator (LO) and master oscillator (MO) frequencies of 1427 MHz and 70 MHz, respectively. The data is acquired at 56 MHz which provides direct I/Q sampling at 1/1.25 of the intermediate frequency (IF) of 70 MHz. The 70 MHz is a legacy frequency based on the RF control module technology used in CEBAF which was developed in the early 1990's.

The receiver cards in the FCC are designed to down convert the nominal 1497 MHz RF signal to 70 MHz, prior to applying the signal to the input of a high speed analog to digital converter. After digital signal processing, the 70 MHz component of output of the digital to analog converter is up-converted to 1497 MHz. This signal is filtered using a 30 MHz filter which rejects the IF and LO signals and is the limiting factor for the output frequency. The receiver card was modified by replacing the printed circuit board mounted band pass filter with two connectors so that it could be used for several applications, such as the 1300 MHz systems being installed as part of the LCLS II infrastructure improvements for the JLAB cryomodule test facility as well as the 1800 MHz chosen for the vertical test area. Other modifications included isolation amplifiers for the LO which allowed us to reduce input signal level for the LO, careful consideration of LO to output isolation, and a reduction of the input signal range.

The standard imbedded firmware on the FCC has algorithms that allow one to operate the system in self-excited loop mode (e.g. frequency tracking), tone mode, closed loop amplitude/phase control and a combination of pulsed mode and self-excited loop. It also has the capability to produce waveform records, and apply digital filters to the internal signals as selected through the

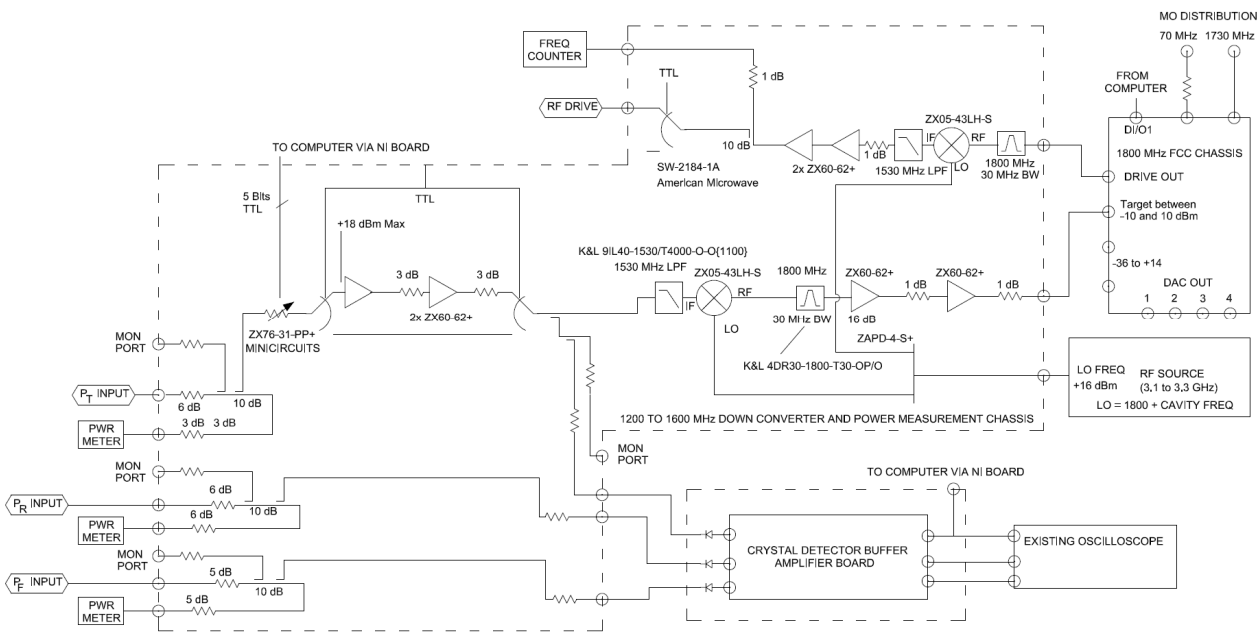

Figure 2: Low Level RF system block diagram.

software interface. These features are available in the standard production firmware and EPICS, which is what is used in the configuration described in this paper.

Frequency Conversion and Instrumentation

The general topology of the frequency conversion and instrumentation systems was the same for the three different types of systems. Figure 2 is the detailed RF bock diagram for the L-band, 1.3 to 1.5 GHz, system. Because we were building such a small number of each type of system, the decision was made to construct it using connectorized commercial off the shelf components. This allowed us the flexibility to make adjustments to the system during the commissioning phase in order to optimize the critical parameters.

One of the trade-offs, when FCC for the accelerator was designed was the number of bits of precision versus the system dynamic range. The design specification for the CEBAF 12 GeV system was full accuracy with a 20 dB dynamic range, which is a factor of ten in cavity gradient. When testing cavities vertically one often needs 50 dB or 60 dB of dynamic range. This is due in part by the desire to test from 0.1 MV/m to 40 MV/m as well as the changes in signal levels when changing from different cavity types or processing methods. For this reason as well as calibration traceability to an outside source, we chose to use commercial RF power meters and frequency counters for making RF measurements and included a variable attenuator switchable amplifier circuit in the RF measurement network.

The approach of using a two-step frequency conversion system was adopted in order to ensure isolation of the LO frequencies and the difference frequency, $F_{LO} - F_{MO}$, with respect to the output signal which is the sum frequency, $F_{LO} + F_{MO}$. If one were to do a single up/down conversion then one would need a bank of 8 bandpass filters in order to cover the 1.2 to 1.6 GHz frequency range. By doing a second up/down conversion using a high side local oscillator signal, the output filter can be reduced to a single low pass filter. Even with this one must carefully select of the mixer and low pass filter used in the output circuit so as to avoid power measurement errors due to the FCC RF signal or up/down conversion LO frequency from leaking through. Using this approach allowed us to build a system that can be operated between 1.2 and 1.6 GHz simply by adjusting one frequency source. A similar low side down conversion approach was taken with the UHF system which had a requirement of operation between 250 MHz and 1 GHz and a final specified range of 50 MHz to 1.3 GHz.

It was not possible to use a low side converter for the 7.3 GHZ system. Thus the output filter for the up converter was a band pass filter with a bandwidth of 200 MHz.

SOFTWARE

The LabView based software used in the vertical test area was originally developed in 1990 [2] and was completely rewritten in 2003. The computer based system measures the RF power, frequency, decay time constants and radiation levels inside the shielded dewar lid. The software processes this information and calculates the cavity gradient, E, loaded-Q, Q_0, field probe-Q, Q_2, etc. and associated errors. It has the capability to optimize the phase, perform guided cable calibrations, auto step the incident power, open and close the SEL, and can be operated in a pulsed RF power mode. The operator is still required to determine if the cavity is overcoupled or undercoupled by observing the reflected power waveform during pulsed operation. This signal, along with the waveform for the forward and transmitted power signals, is routed to an oscilloscope which provides the operators prompt feedback on the time domain behaviour of the system.

The transmitted power signal is also routed to an ADC in the computer so that it can be used for determining the 1/e power decay time constant, τ, which is used for determining the system loaded-Q. An external RF source and pair of power meters are used to measure the amplified crystal detector voltage under different operating conditions. This data is used in a linearization algorithm to improve the accuracy of the decay measurement. Loop phase offsets are measured for the transmitted power input attenuator and amplifier as part of the system commissioning. This data is used to provide a phase offset when the components are switched into or out of the system.

Error Analysis

One major change in the software is the calculation of the errors associated with a given measurement. The error calculations that were developed in 1990 were done using a simple "chain" rule method where, for example, the error in the reflection coefficient is calculated, then that error is used to calculate the error β^*, etc. [4]. A more accurate approach is to derive the equation for *E, Qo*, etc. in terms of measurable parameters such as incident power, reflected power, decay time constant; take the partial derivative of said equations and apply the errors associated with measurable parameters. For the decay measurement, the equations for Q_0, E and Q_2 can be reduced to:

$$Q_0 = Q_0 = 4\pi f_0 \tau \frac{P_f + C_\beta \sqrt{P_r P_f}}{P_f - P_r - P_t}$$

$$E = \sqrt{4\pi f_o \tau \left(P_f + C_\beta \sqrt{P_r P_f}\right) \frac{(r/Q)}{L}}$$

$$Q_2 = 4\pi f_0 \tau \frac{P_f + C_\beta \sqrt{P_r P_f}}{P_t}$$

Where P_f is the measured incident or forward power at the cavity, P_r is the reflected power at the cavity, P_t is the transmitted or field probe power at the cavity, τ is the 1/e decay time constant for the probe power after the incident power is removed and (r/Q)/L is the normalized shunt

ISBN 978-3-95450-178-6

impedance divided by the length of the cavity which for elliptical cavities is defined the iris to iris length of the cavity.

The general equation for error of a function of x, y, and z where the errors in x, y and z are Gaussian and not correlated is:

$$\Delta(f(x,y)) = \sqrt{\left(\frac{\partial f}{\partial x}\Delta x\right)^2 + \left(\frac{\partial f}{\partial y}\Delta y\right)^2}$$

After several pages of math applying this to the Q_0, Q_2, and E equations leads to the following:

$$\Delta Q_0 = Q_0 \sqrt{\left(\left(\frac{(2P_f + C_\beta\sqrt{P_f P_r})}{2(P_f + C_\beta\sqrt{P_r P_f})} - \frac{P_f}{P_{Disp}}\right)\frac{\Delta P_f}{P_f}\right)^2 + \left(\left(\frac{(C_\beta\sqrt{P_r P_f})}{2(P_f + C_\beta\sqrt{P_r P_f})} + \frac{P_r}{P_{Disp}}\right)\frac{\Delta P_r}{P_r}\right)^2 + \left(\frac{\Delta\tau}{\tau}\right)^2}$$

$$\Delta Q_2 = Q_2 \sqrt{\left(\frac{(2\sqrt{P_f} + C_\beta\sqrt{P_r})}{2(\sqrt{P_f} + C_\beta\sqrt{P_r})}\frac{\Delta P_f}{P_f}\right)^2 + \left(\frac{\sqrt{P_r}}{2(\sqrt{P_f} + C_\beta\sqrt{P_r})}\frac{\Delta P_r}{P_r}\right)^2 + \left(\frac{\Delta P_t}{P_t}\right)^2 + \left(\frac{\Delta\tau}{\tau}\right)^2}$$

$$\Delta E = \frac{E}{2}\sqrt{\left(\frac{(2P_f + C_\beta\sqrt{P_f P_r})}{2(P_f + C_\beta\sqrt{P_r P_f})}\frac{\Delta P_f}{P_f}\right)^2 + \left(\frac{\sqrt{P_r}}{2(\sqrt{P_f} + C_\beta\sqrt{P_r})}\frac{\Delta P_r}{P_r}\right)^2 + \left(\frac{\Delta\tau}{\tau}\right)^2}$$

One metric of a specific cavity measurement is the system beta, this is a measure of the percentage of the incident power which goes into the cavity wall losses added to the amount that escapes through any other ports such as the field probe ports. In the case where all of the power goes into the structure and there is no reflected power, beta is equal to one. Beta is given by:

$$\beta = \frac{1 + C_\beta\sqrt{P_r/P_f}}{1 - C_\beta\sqrt{P_r/P_f}}$$

Here C_β is one if the cavity is overcoupled and minus-one if the cavity is undercoupled. Figure 3 shows the error in the calculated gradient, E, cavity quality factor, Q_0, and field probe-Q, Q_2, of a cavity as a function of β. The assumed measurement errors used for these results were 10% error in P_f, P_r and P_t and a 3% error in the RF power decay time constant, τ.

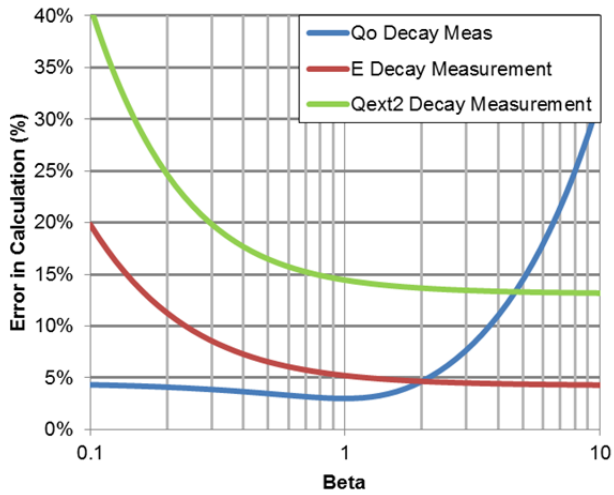

Figure 3: Decay measurement errors in Q_0, E and Q_2 as a function of beta.

When performing CW measurements one uses the Q_2 value calculated using the decay measurement method along with the P_f, P_r and P_t in order to calculate the values of E and Q_0. The errors in E are straightforward. There is an error associated with the Q_2 value calculated based on a decay measurement and during CW measurements E is given by:

$$E = \sqrt{Q_2 P_t \frac{(r/Q)}{L}}$$

Thus, any cable, coupler, etc. calibration errors in Pt are already included in the errors in Q_2. This means that the only additional error is the linearity error associated with P_t, or:

$$\Delta E = \frac{E}{2}\sqrt{\left(\frac{\Delta Q_2}{Q_2}\right)^2 + \left(\frac{\Delta P_{tLin}}{P_t}\right)^2}$$

Here $\Delta P_{tlin}/P_t$ is the linearity error in the transmitted power meter and $\Delta Q_2/Q_2$ is the error in Q_2 when it was calculated using a decay measurement. The effect of this is that E has a constant fractional error that is slightly higher than the gradient at which Q_2 was calculated.

The complication in calculating the errors in CW Q_0 measurements is because there are a number of systematic errors in the RF power measurements which are the same as those present when calculating Q_2 using the decay method. However, there are errors such as power meter linearity and changes in directional coupler properties as a function of beta, which will introduce added uncertainty when doing CW measurements. An equation that describes this is:

$$Q_0 = \frac{4\pi f_0 \tau P_{tm}\left(C_f P'_{fm} + C'_\beta\sqrt{C_f C_r P'_{fm} P'_{rm}}\right)}{(C_f P_{fm} - C_r P_{rm} - C_t P_{tm})P'_{tm}}$$

Here C_x is the calibration for the respective measurement; P_{xm} is the power measurement including any amplitude correlated errors; and the primed notation indicates the values used in determining the specific Q_2 value used for

the CW measurements as measured during the decay measurement. Applying the differential equation based error calculation to the above equation leads to:

$$\frac{\Delta Q_0}{Q_0} = \sqrt{\begin{aligned}&\left(\left[\frac{2P_f' + C_\beta'\sqrt{P_f'P_r'}}{2\left(P_f' + C_\beta'\sqrt{P_f'P_r'}\right)} - \frac{P_f}{P_f - P_r - P_t}\right]\frac{\Delta C_f}{C_f}\right)^2 + \\ &+\left(\frac{P_t}{P_f - P_r - P_t}\frac{\Delta C_t}{C_t}\right)^2 + \left(\frac{\Delta\tau}{\tau}\right) \\ &+\left(\left[\frac{C_\beta'\sqrt{P_f'P_r'}}{2\left(P_f' + C_\beta'\sqrt{P_f'P_r'}\right)} + \frac{P_r}{P_f - P_r - P_t}\right]\frac{\Delta C_r}{C_r}\right)^2 \\ &+\left(\left[\frac{P_f}{(P_f - P_r - P_t)}\right]\frac{\Delta P_{fm}}{P_{fm}}\right)^2 \\ &+\left(\left[\frac{P_r}{(P_f - P_r - P_t)}\right]\frac{\Delta P_{rm}}{P_{rm}}\right)^2 \\ &+\left(\left[1 + \frac{P_t}{(P_f - P_r - P_t)}\right]\frac{\Delta P_{tm}}{P_{tm}}\right)^2\end{aligned}}$$

Here the $\Delta C_x/C_x$ terms are the fixed calibration errors that are the same in both decay and CW measurements; the $\Delta P_{xm}/P_{xm}$ terms are the RF power measurements which include the nonlinearities, etc. which could lead to variations between CW and decay measurements and the primed variables are the actual values, and thus constant when doing the derivatives

Figure 4 shows the resultant errors in a set of CW Q_0 measurements as a function of CW beta. Each curve represents the effect of the errors in Q_2 which was calculated using a decay measurement with the indicated beta. For this graph the $\Delta C_x/C_x$ values were 10%, the $\Delta P_{xm}/P_{xm}$ values were 5% and $\Delta\tau/\tau$ values were 3%. As expected, the results indicate that the most accurate values of CW Q_0 occur when the decay measurements are made with beta less than 1 and that the CW errors increase as the beta values increase or decrease about the value of 1.

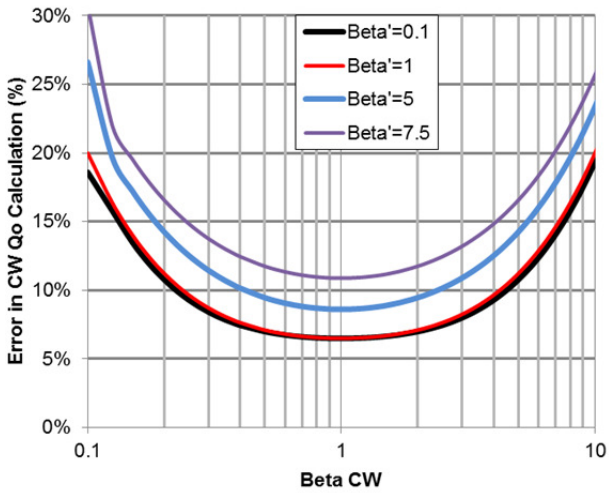

Figure 4: Error in CW Q_0 calculations for various values of Q_2 where β' is the beta value at which Q_2 was calculated when doing a decay measurement.

CONCLUSION

This details of the upgrades to the VTA production RF systems have been described as well as improvements to the error calculations that will be implemented when the two L-band systems are commissioned. The UHF variant of the system has been operational for the past year, and we have used it to test several cavities at frequencies ranging from 325 MHz to 850 MHz. It is simple to use and reduces the time required to test a cavity. The 1.2–1.6 GHz and 7 GHz systems are currently being fabricated, and, along with the RF switching network, they will be installed in the coming months as resources become available. A revised set of error calculations has been developed and is being deployed with the new installations.

REFERENCES

[1] C. Reece, et al., "A Closed Cycle Cryogenic System for Testing Superconducting RF Cavities," PAC 1991, June 1991, p 2325, http://www.JACoW.org

[2] C. Reece, et al., "An Automated RF Control and Data Acquisition System for Testing Superconducting RF Cavities," PAC 1991, June 1991, p 1508, http://www.JACoW.org

[3] C. Hovater, et al., "Status of the CEBAF Energy Upgrade RF control System", Linac2010, Sept. 2010, p 280, http://www.JACoW.org

[4] T. Powers, "Theory and Practice of Cavity RF Test Systems," Tutorial at SRF Workshop 2005, July 2005, http://www.lns.cornell.edu/public/SRF2005/pdfs/SuP02.pdf

.

ISBN 978-3-95450-178-6